

Adaptive neuro-fuzzy estimation of autonomic nervous system parameters effect on heart rate variability

D. Petković · Ž. Čojbašić

Received: 12 February 2011 / Accepted: 3 May 2011
© Springer-Verlag London Limited 2011

Abstract Heart rate signal can be used as certain indicator of heart disease. Spectral analysis of heart rate variability (HRV) signal makes it possible to partly separate the low-frequency (LF) sympathetic component, from the high-frequency (HF) vagal component of autonomic cardiac control. Here, we used two important features to characterize the nonlinear fluctuations in the heart variability signal (HRV): cardiac vagal index (CVI) and cardiac sympathetic index (CSI) which indicates vagal and sympathetic function separately. This article presents a methodology for analyzing the influence of CVI and CSI on heart rate variability spectral patterns—low-frequency (LF) and high-frequency (HF) spectral bands and LF/HF ratio. An adaptive neuro-fuzzy network is used to approximate correlation between these two features and spectral patterns. This system is capable to find any change in ratio of features and spectral patterns of heart rate variability signal (HRV) and thus indicates state of both parasympathetic and sympathetic functions in newly diagnosed patients with heart diseases.

Keywords Heart rate · Neuro-fuzzy · Nervous system · Poincare plot · Spectral frequency

D. Petković (✉) · Ž. Čojbašić
University of Niš, Mechanical Engineering Faculty,
Aleksandra Medvedeva 14, 18000 Niš, Serbia
e-mail: dalibortc@gmail.com

D. Petković · Ž. Čojbašić
Department of Mechatronics and Control,
University of Niš, Nis, Serbia

1 Introduction

Heart rate variability (HRV) is useful signal for understanding the status of the autonomic nervous system (ANS) [1]. HRV analysis involves three major procedures. After the ECG recording is digitized, the R waves of the ECG are detected through a QRS complex detection algorithm such as Pan-Tomkins QRS detection algorithm [2]. Then, the RR interval time series is obtained from the time interval between consecutive R waves. Finally, the time-domain, frequency-domain, and nonlinear HRV-related parameters can be computed by analyzing the time series [3, 4].

Numerous methods of quantifying HRV have been proposed [5–7]. Because the HRV signals are highly nonlinear and complex, analysis of these signals using linear statistics does not characterize the nonlinearity or the chaoticity of the signals [7]. Since HRV signals are regulated by complex mechanisms (ANS), it is rationale presume that HRV also contains nonlinear properties. One simple and easy measure to visualize the nonlinear properties of RR interval series data is the Poincare plot [7–10]. It is graphic representation of the correlation between consecutive RR interval series and characterizes current status of ANS. ANS is a part of nervous system that non-voluntary controls all organs and systems of the body. ANS has its central and peripheral components accessing all internal organs.

There are two branches of the ANS system—sympathetic and parasympathetic (vagal) nervous system that always work as antagonist in their effect on target organs. The sympathetic nervous system stimulates organs' functioning. An increase in sympathetic stimulation causes increase in HR. In contrast, the parasympathetic nervous system inhibits functioning of those organs. The actual balance between them is constantly changing in an attempt

to achieve optimum considering all internal and external stimuli. HRV analysis provides ability to assess overall cardiac health and the state of ANS responsible for regulating cardiac activity. The normal variability in HR is due to autonomic neural regulation of the heart. Increased sympathetic nervous system or diminished parasympathetic nervous system results in cardio-acceleration and vice versa. The both branches of ANS operate at distinct frequencies [11]. Spectral analysis of HRV was applied in order to obtain noninvasive indices of sympathetic and parasympathetic regulation [12, 13]. Research studies [3, 4] have demonstrated that the high-frequency (HF: 0.15–0.40 Hz) power of HRV is an index associated with parasympathetic activity, while the low-frequency (LF: 0.04–0.15 Hz) power of HRV is an index associated with both sympathetic and parasympathetic activities. Moreover, the LF/HF ratio has been considered to reflect sympathetic modulations or sympathovagal balance [14–17].

Tochi et al. [18] have recommended two measures, the cardiac vagal index (CVI) and the cardiac sympathetic index (CSI), which indicate vagal and sympathetic function separately. These two indices have found to be more reliable than those obtained by the other methods. Che-Wei Lin, Jeen-Shing Wang, and Pau-Choo Chung [19] have developed methodology for mining physiological condition from HRV analysis using CVI and CVS indexes.

In this work, an attempt is made to retrieve correlation between indexes that are related to ANS—LF, HF, and LF/HF and indexes that qualify the nonlinearity and the chaoticity of the HRV signal—CVI and CSI. That system should be able to show which of the two ANS parts are more active for certain therapy [20–24] and to estimate ANS influence on HRV. Adaptive neuro-fuzzy inference system (ANFIS) [25] is used for system modeling where CSI and CVI indexes are inputs and spectral indexes LF, HF, and LF/HF are outputs. ANFIS is a soft computing methodology. Yardimci [26] demonstrates the possibilities of applying soft computing (SC) to medicine-related problems. Some of these SC methodologies have already been applied for ECG and HRV signals processing for classification [29, 32, 34–37, 39], analysis [30], recognition [31, 35], diagnosis [33], and prediction [38]. ANFIS has been used only for the classification of ECG signals [27, 28].

2 Material and method

ECG data for the analysis were obtained from PhysioBank database. For this work, MIT-BIH Arrhythmia Database was used which contains 48 half-hour ECG recordings. The subjects were 25 men aged 32–89 years, and 22 women aged 23–89 years. Each of the 48 records is slightly over 30 min long. The signals group is intended to serve as a

representative sample of the variety of waveforms and artifact that an arrhythmia detector might encounter in routine clinical use and some records were chosen to include complex ventricular, junctional, and supraventricular arrhythmias and conduction abnormalities. The recordings were digitized at 360 samples per second per channel with 11-bit resolution over a 10-mV range.

The procedure involves three major steps. The first step is to record and digitize ECG signals. After the ECG recording is digitized, the R waves of the ECG are detected through a QRS complex detection algorithm such as Pan-Tomkins QRS detection algorithm [2]. The RR interval time series is obtained from time between consecutive R waves. Then, the HRV-related parameters are computed in frequency-domain LF, HF, and LF/HF and nonlinear parameters cardiac vagal index (CVI) and cardiac sympathetic index (CVS).

3 Input and output parameters

Input parameters are CVI and CSI, and outputs are spectral indexes LF, HF, and LF/HF for adaptive neuro-fuzzy inference system.

3.1 Cardiac vagal index (CVI) and cardiac sympathetic index (CSI)

The Poincare plot is a two-dimensional nonlinear plot, which was originally designed for the application in metrology and has recently been applied in the field of electrophysiology. When the sequence of the consecutive RR interval is expressed by I_1, I_2, \dots, I_n , the Poincare plot is constructed by plotting I_{k+1} against I_k ($k = 1, 2, \dots, n - 1$). Figure 1 shows the Poincare plot for one of the subjects. In this plot, the RR fluctuation is transformed into the points distributed on a two-dimensional plane which form an ellipsoid configuration.

We calculated two components of the RR fluctuations from Poincare plot such as this one: the length of the transverse axis SD1 which is vertical line $I_k = I_{k+1}$, and that of the longitudinal axis SD2 which is parallel with the line $I_k = I_{k+1}$. When two adjacent intervals I_m and I_{m+1} in the sequence differ greatly (large beat-to-beat variation), the point (I_m, I_{m+1}) is plotted distant from the line $I_k = I_{k+1}$ on the plane, resulting in large SD1. On the other hand, when the fluctuation is great but continuous (large amplitude, but small beat-to-beat variation), the plotted points are distributed widely but along the line $I_k = I_{k+1}$, resulting in large SD2 and small SD1. Thus, the two components reflect different aspects of the RR fluctuation. SD1 describes short-term variability, and SD2 describes long-term variability. SD1 is influenced by both the sympathetic

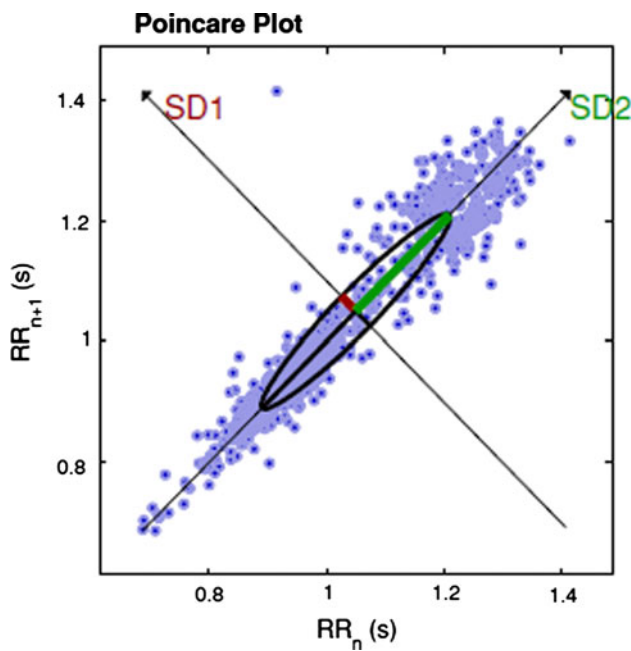


Fig. 1 Poincare plot geometry of a subject

and parasympathetic nervous system, whereas SD2 is affected only by the parasympathetic nervous system.

Tochi et al. [18] have been showed that product $SD1 \times SD2$ is a sensitive index of cardiac parasympathetic function, which is not affected by sympathetic activity. Since the measure $SD1 \times SD2$ showed a wide range of values, a logarithm was employed to accommodate the measure to statistical analysis. Thus, the component $\log_{10}(SD1 \times SD2)$ is influenced only by vagal nervous system. Tochi termed this measure the “cardiac vagal index” (CVI). According to Tochi, $SD1/SD2$ ratio is an index of cardiac sympathetic function, which is not affected by vagal activity, and this measure is termed as “cardiac sympathetic index” (CSI).

3.2 Frequency-domain parameters

Frequency-domain measures pertain to HR variability at certain frequency ranges associated with specific physiological processes. Before frequency-domain analysis is performed, all abnormal heartbeats and artifacts must be detected and removed, and then cardiogram (sequence of RR intervals) must be resampled to make it as if it a regularly sampled signal. A standard spectral analysis routine is applied to such modified recording, and the following parameters evaluated on 5-min time interval: total power (TP), high frequency (HF), low frequency (LF), and very low frequency (VLF). When long-term data are evaluated, an additional frequency band is derived—ultra low frequency. The TP is net effect of all possible

physiological mechanisms contributing in HR variability that can be detected in 5-min recording.

The HF power spectrum is in the range from 0.15 to 0.4 Hz, and this band reflects parasympathetic (vagal) tone and fluctuations caused by respiration known as respiratory sinus arrhythmia. The LF spectrum is in the range from 0.04 to 0.15 Hz, and this band reflects both sympathetic and parasympathetic tone. The VLF power spectrum is evaluated in the range from 0.0033 to 0.04 Hz. With longer recordings, it is considered representing sympathetic tone. The ULF power spectrum is evaluated below 0.0033 Hz. The LF/HF ratio is used to indicate balance between sympathetic and parasympathetic tone. A decrease in this score might indicate either increase in parasympathetic or decrease in sympathetic tone. It must be considered together with absolute values of both LF and HF to determine what factor contributes in autonomic imbalance.

The frequency-domain analysis is traditionally performed by means of Fast Fourier Transformation (FFT). This method is simple in calculation for steady-state process and fair representation of all frequency-domain of HRV scores for at least 5-min data that should be collected. Some most recent studies implemented an alternative way to estimate power spectrum of HRV. It is based on autoregression methods (AR). One of its major advantages is that it does not require to have analyzed data series to be in steady state. Thus, any HRV data can be analyzed and fair HRV information still derived. Such analyses can be also performed at relatively shorter time intervals (less than 5 min) without missing meaningful HRV information. AR method is sensitive to rapid changes in HR properly showing tiny changes in autonomic balance. The drawback of this approach is a necessity to perform massive calculations to find best order of autoregression model.

In this work, the autoregressive method is applied for spectral analysis of HRV signals. The estimation of AR parameters can be done easily by solving some linear equations. The input and output parameters scopes were shown in Table 1.

4 Adaptive neuro-fuzzy inference system for function approximation

Jang [25] describes adaptive neuro-fuzzy inference system (ANFIS), which can be used for classification,

Table 1 Input and output parameters scopes

HF	$50,213.2 \pm 50,186.8$
LF	$62,170.8 \pm 62,129.2$
LF/HF	1.9 ± 1.83
CVI	3.1891 ± 2.6749
CSI	4.0225 ± 1.4365

approximation of highly nonlinear functions, online identification in discrete control system and to predict a chaotic time series. Jang proves the resulting fuzzy inference system has unlimited approximation power to match any nonlinear functions arbitrarily well on compact set and proceed this in a descriptive way.

In this work, we used first-order Sugeno model with two inputs. We formed three ANFIS models because there are three outputs LF, HF, and LF/HF and we used fuzzy if-then rules of Takagi and Sugeno's type [90]:

if x is A_1 and y is B_1 then $f_1 = p_1x + q_1y + r_1$

In the first layer, every node is an adaptive node with a node function $O = \mu_{A_i}(x)$ where $\mu_{A_i}(x)$ is membership function. In this work, we chose to be bell shaped with maximum equal to 1 and minimum equal to 0, such as

$$\mu_{A_i}(x) = \frac{1}{1 + \left[\left(\frac{x-c_i}{a_i} \right)^2 \right]^{b_i}}$$

where $\{a_i, b_i, c_i\}$ is the parameter set and in this layer are referred to as premise parameters. X is the input to node in this layer, and it is CVI and CSI.

Every node in the second layer is nonadaptive, and this layer multiplies the incoming signals and sends the product out like $w_i = \mu_{A_i}(x)\mu_{B_i}(y)$. Each node output represents the firing strength of a rule.

The third layer is also nonadaptive, and every node calculates the ratio of the rule's firing strength to the sum of all rules' firing strength like $\bar{w}_i = \frac{w_i}{w_1+w_2}$, $i = 1, 2$. The outputs of this layer are called normalized firing strengths.

Every node in the fourth layer is adaptive node with node function $O_i^4 = \bar{w}_i f_i = \bar{w}(p_i x + q_i y + r_i)$ where $\{p_i, q_i, r_i\}$ is parameter set and in this layer are referred to as consequent parameters.

The single node in the fifth layer is not adaptive, and this node computes the overall output as the summation of all incoming signals

$$O_i^4 = \sum_i \bar{w}_i f_i = \frac{\sum_i w_i f_i}{\sum_i w_i}$$

This type of an adaptive network is functionally equivalent to a type-3 fuzzy inference system. We applied the hybrid learning algorithms to identify the parameters in the ANFIS architectures. In the forward pass of the hybrid learning algorithm, functional signals go forward till layer 4 and the consequent parameters are identified by the least squares estimate. In the backward pass, the error rates propagate backward and the premise parameters are updated by the gradient descent. The ANFIS architectures for all three outputs are shown in Fig. 2.

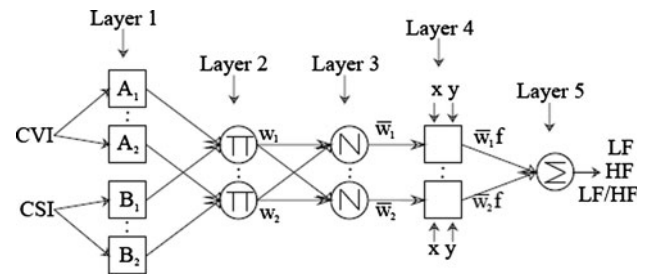


Fig. 2 ANFIS network used for approximation. These three outputs make three ANFIS models

5 Results

In this paper, we extracted 48 ECG recordings from MIT-BIH Arrhythmia Database. All of these signals were used for ANFIS training because the group serves as a representative sample of the variety of waveforms and artifacts that an arrhythmia detector might encounter, and these data contain all the necessary representative features so we do not need for ANFIS testing and validating. The main goal was to find optimal ANFIS parameters where final decision surfaces in all three cases are thorough positive—no negative parts, because spectral parameters LF, HF, and LF/HF are always positive. After several testings, we have found optimal ANFIS parameters that are shown in Table 2.

Table 2 General characteristics of ANFIS architectures which was found to be optimal

Inputs	Output	Membership functions #	Membership function type	Mean square error
CVI & CSI	HF	21	Bell-shaped	0.0015734
CVI & CSI	LF	24	Bell-shaped	0.0027135
CVI & CSI	LF/HF	24	Bell-shaped	1.3887×10^{-7}

Results for MIT-BIH Arrhythmia Database

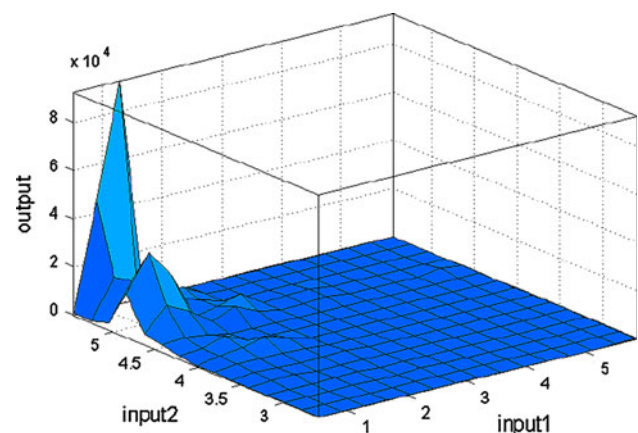


Fig. 3 Final decision surface for input1 = CVI, input2 = CVS, and output = HF

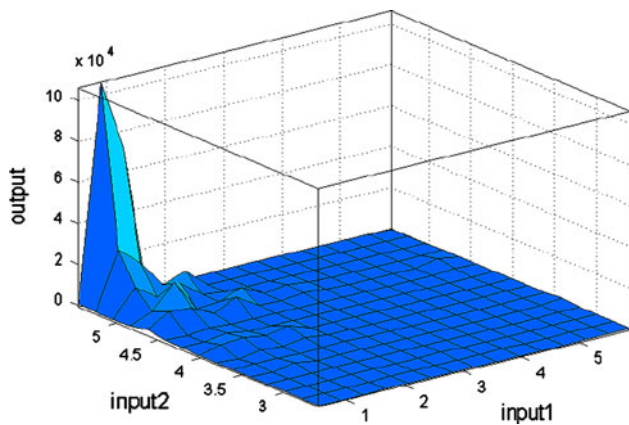


Fig. 4 Final decision surface for input1 = CVI, input2 = CVS, and output = LF

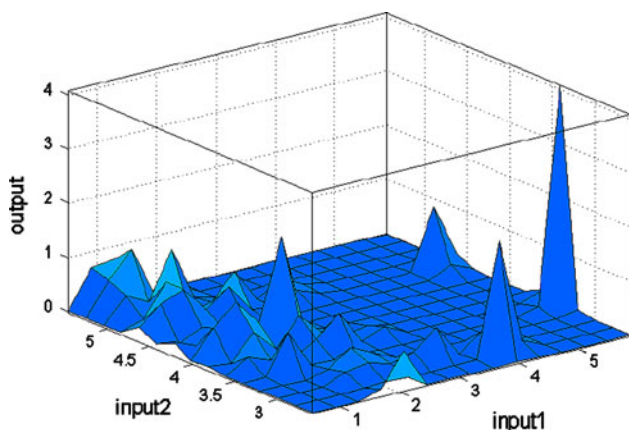
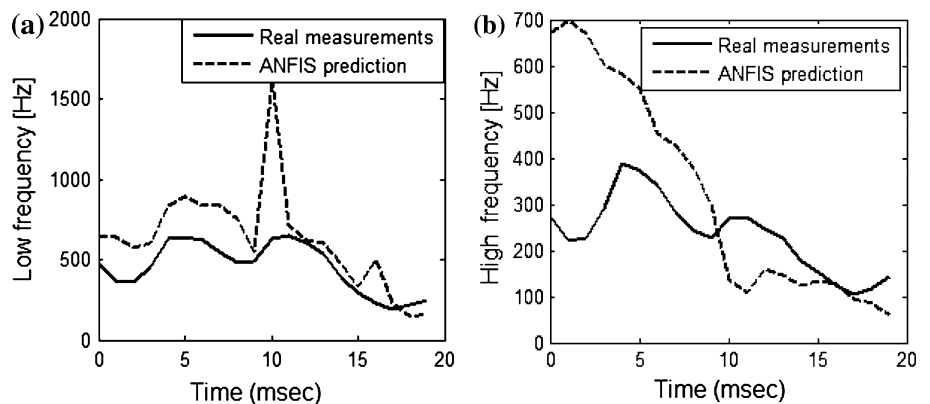


Fig. 5 Final decision surface for input1 = CVI, input2 = CVS, and output = LF/HF

The mean squared errors (MSE) are acceptable for this purpose of research. The MSE for HF and LF are in order 10^{-3} , and for ratio LF/HF even 10^{-7} . Minimal number of membership functions for which is thorough final decision surfaces positive are shown in Table 2. This ANFIS algorithm is useful for the input and output parameters in range shown in Table 1. For the wider input/output parameters

Fig. 6 Comparisons between real measurements of low and high frequency of HRV and ANFIS predictions



range, we must add ECG recordings with new features and abnormalities. The final decision surfaces after training were shown in Figs. 3, 4, and 5.

Figure 6 shows the real measurements of HRV activity and one predicted by ANFIS. This system could detect automatic nervous system branches activity in real time. There are differences between predicted and real curves. It is clear for better prediction that we need more membership functions and training epochs. The ANFIS network was trained with two membership functions, 16 fuzzy rules and 104 total number of parameters.

6 Conclusion

One of the most important features of the ANFIS networks is real-time detection and online identification of the automatic nervous system (ANS) branches activity. It is useful for ANS treatment if the branches did not have optimal state characteristics. In this paper, HRV nonlinear parameters are used as a reliable indicator of ANS diseases.

Heart rate signal can be used as certain indicator of heart disease. We have used the spectral analysis for the ANS monitoring—sympathetic activity increase/decrease and parasympathetic activity increase/decrease. It is an indicator of HRV activity. We have used cardiac vagal index (CVI) and cardiac sympathetic index (CSI) which indicate vagal and sympathetic function separately. It is found to be more reliable than those obtained by the other methods. Those parameters are in reasonable ranges as the measures to statistical analysis. For simplicity, we have not applied the ANFIS validating and testing because the signals group is intended to serve as a representative sample of the variety of waveforms and artifact. Addition of the new signals increases training time for the ANFIS models, and it is not insignificant. Therefore, we must choose optimal number and type of ECG recordings for the new databases, which will cover wider variations spectra of ECG abnormalities.

Future demands are increasing the input parameters ranges without the ANFIS training time increasing. One of

the possible solutions is to create three different ECG group recordings. Each of group will be used for ANFIS training, validation, and testing separately. The three ECG groups will cover different variation of ECG recordings, and the main goal will be determining optimal ANFIS parameters which approximate all the three ECG groups. This model has a drawback. It is larger mean squared error than the recommended ANFIS model in this paper, but the ANIFS time training would be much shorter in this new model.

References

- Zhong Y, Wang H, Ju KH, Jan KM, Chon KH (2004) Nonlinear analysis of the separate contributions of autonomic nervous systems to heart rate variability using principal dynamic modes. *IEEE Trans Biomed Eng* 51:255–262
- Pan J, Tompkins JW (1985) A real-time QRS detection algorithm. *IEEE Trans Biomed Eng* 32:230–255
- Malik M (1996) Heart rate variability: standards of measurement, physiological interpretation, and clinical use. *Eur Heart J* 17:354–381
- Berntson GG, Bigger JT et al (1997) Heart rate variability: origins, methods, and interpretative caveats. *Psychophysiology* 34:623–648
- Pincus MS (1991) Approximate entropy as a measure of system complexity. *Proc Nat Acad Sci* 88:2297–2301
- Xinbao N, Chunhua B, Jun W, Ying C (2006) Research progress in nonlinear analysis of heart electric activities. *Chin Sci Bull* 51:385–393
- Chunhua B, Xinbao N (2004) Nonlinearity degree of short-term heart rate variability signal. *Chin Sci Bull* 49:530–534
- Mourot L, Bouhaddi M, Perrey S et al (2004) Quantitative Poincare plot analysis of heart rate variability: effect of endurance training. *Eur J Appl Physiol* 91:79–87
- Lerma C, Infante I, Groves HP, Jose MV (2003) Poincare plot indexes of heart rate variability capture dynamic adaptations after haemodialysis in chronic renal failure patients. *Clin Physiol Func Im* 23:72–80
- Addio GD, Pinna GD, Rovere MTL, Maestri R et al (2001) Prognostic value of Poincare plot indexes in chronic heart failure patients. *Comput Cardiol* 28:57–60
- Chiu HW, Wang TH, Huang LC et al (2003) The influence of mean heart rate on measures of heart rate variability as markers of autonomic function: a model study. *Med Eng Phys* 25:475–481
- Basano L, Canepa F, Ottonello P (1998) Real-time spectral analysis of HRV signals: an interactive and user-friendly PC system. *Comput Methods Programs Biomed* 55:69–76
- Wu GQ, Arzeno MN, Shen LL et al (2009) Chaotic signatures of heart rate variability and its power spectrum in health, aging and heart failure. *PLoS One Public Library Sci* 4:2
- Busek P, Vankova J, Opavsky J et al (2005) Spectral analysis of heart rate variability in sleep. *Physiol Res* 54:369–376
- Groome JL, Mooney MD, Bentz SL, Singh PK (1994) Spectral analysis of heart rate variability during quiet sleep in normal human fetuses between 36 and 40 weeks of gestation. *Early Hum Dev* 38:1–10
- Colak HO (2009) Preprocessing effects in time-frequency distributions and spectral analysis of heart rate variability. *Dig Sig Proc* 19:731–739
- Khandoker AH, Jelinek HF, Moritani T, Palaniswami M (2010) Association of cardiac autonomic neuropathy with alteration of sympatho-vagal balance through heart rate variability analysis. *Med Eng Phys* 32:161–167
- Toichi M, Sugiura T, Murai T, Sengoku A (1997) A new method of assessing cardiac autonomic function and its comparison with spectral analysis and coefficient of variation of R-R interval. *J Aut Nerv Syst* 62:79–84
- Lin CW, Wang JS, Chung PC (2010) Mining physiological conditions from heart rate variability analysis. *IEEE Comput Intell Mag* 5:50–58
- Apfelbaum JD, Caravati EM, Kerns WP, Bossart PJ, Larsen G (1995) Cardiovascular effects of carbamazepine toxicity. *Ann Emerg Med* 25:631–635
- Meneses ASJ, Moreira HG, Daher MT (2004) Analysis of heart rate variability in hypertensive patients before and after treatment with angiotensin II-converting enzyme inhibitors. *Arquivos Brasileiros de Cardiologia* 83:169–172
- Lado MJ, Vila XA, Rodriguez LL, Mendez AJ, Olivieri DN, Felix P (2009) Detecting sleep apnea by heart rate variability analysis: assessing the validity of databases and algorithms. *J Med Syst* 33:1–9
- Persson H, Ericson M, Tomson T (2007) Heart rate variability in patients with untreated epilepsy. *Seizure* 16:504–508
- Halliloglu O, Ocuyaz C, Mert E, Makharoblidze K (2008) Effects of antiepileptic drug therapy on heart rate variability in children with epilepsy. *Epilepsy Res* 79:49–54
- Jang JSR (1993) ANFIS: adaptive-network-based fuzzy inference system. *IEEE Trans Syst Man Cybern* 23:665–685
- Yardimci A (2009) Soft computing in medicine. *Appl Soft Comput* 9:1029–1043
- Ubeyli ED (2009) Adaptive neuro-fuzzy inference system for classification of ECG signals using Lyapunov exponents. *Comput Method Prog Biomed* 93:313–321
- Nazmy TM, El-Messiry H, Al-Bokhity B (2009) Adaptive neuro-fuzzy inference system for classification of ECG signals. *J Theor Appl Inform Tech* 12:71–76
- Rajendra UA, Subbanna PB, Iyengar SS, Rao A, Dua S (2003) Classification of heart rate data using artificial neural network and fuzzy equivalence relation. *Pattern Recogn* 36:61–68
- Ubeyli ED (2010) Recurrent neural networks employing Lyapunov exponents for analysis of ECG signals. *Exp Syst Appl* 37:1192–1199
- Maglaveres N, Stamkopolulos T, Diamantaras K, Pappas C, Srintzis M (1998) ECG pattern recognition and classification using non-linear transformations and neural networks: a review. *Int J Med Inform* 52:191–208
- Ozbay Y, Tezel G (2009) A new method for classification of ECG arrhythmias using neural network with adaptive activation function. *Digi Sig Proc* 20:1040–1049
- Hosseini HG, Luo D, Reynolds KJ (2006) The comparison of different feed forward neural network architectures for ECG signal diagnosis. *Med Eng Phys* 28:372–378
- Ceylan R, Ozbay Y, Karlik B (2009) A novel approach for classification of ECG arrhythmias: type-2 fuzzy clustering neural network. *Exp Syst Appl* 36:6721–6726
- Osowski S, Markiewicz T, Hoai LT (2009) Recognition and classification system of arrhythmia using ensemble of neural networks. *Measurement* 41:610–617
- Anuradha MB, Reddy VCV (2009) Cardiac arrhythmia classification using fuzzy classifiers. *J Theor Appl Inform Tech* 4:353–359
- Mohammadzadeh-Asl B, Setarehdan SK (2006) Neural network based arrhythmia classification using heart rate variability signal. In: 14th European signal processing conference
- Patil SB, Kumaraswamy YS (2009) Intelligent and effective heart attack prediction system using data mining and artificial neural network. *Eur J Sci Res* 31:642–656
- Annuradha B, Reddy VCV (2008) ANN for classification of cardiac arrhythmias. *ARPN J Engin Appl Sci* 3:1–6